Biangular Reflectance for an Absorbing and Isotropically Scattering Medium

J. A. Roux* and A. M. Smith†
University of Mississippi, University, Mississippi

A comparison between theory and actual data is presented for the biangular reflectance of a thin cryodeposit formed on a cryogenically cooled substrate. The analytical model employed the discrete ordinate formulation to the radiative transport equation, and a numerical finite difference scheme was employed for solution. The participating medium was considered to be an absorbing and isotropically scattering medium bounded by a semitransparent refracting and reflecting top interface and a specular (Fresnel) opaque substrate. Because these deposits are highly scattering in the solar wavelength region, the results are presented for an albedo value of unity.

Introduction

THE state of analytical modeling[1-13] for radiative transfer in one-dimensional situations has become quite good. The real test of any analytical model is how well the model agrees with actual experimental data. Many papers have been written where the incident radiation has been modeled as diffusely distributed. Hottel et al.[3] have modeled the case of collimated incident radiation with Fresnel interfaces and various phase functions. In Ref. 3, the governing equations were solved by an eigenvalue/eigenvector approach. In addition, the influence of Gaussian quadrature order on computational accuracy was shown. Biangular reflectance and transmittance distributions were presented, but no comparison was presented for analytical model verification. The first objective of this paper was to present a comparison between numerical solution to the radiative transport equation and existing biangular reflectance data.[14] The data and analytical model both correspond to a radiatively participating medium for which the refractive index is greater than unity. The reflectance data correspond to cryodeposits formed on cryogenically cooled wall and floor panels of a thermal vacuum chamber.[15] These deposits cause the initially black paint reflectance[15] to increase and, hence, cause a biangular scattering of the incident collimated radiation. The radiative properties (absorption and scattering coefficients) from a previous work[16] were used in these calculations. These radiative properties were determined from an analytical model employing diffusely incident radiation and isotropic scattering. The experimental data[14] correspond to cryopumped CO_2 and are considered to have a refractive index of 1.4. Typical vacuum chamber pressure would be 1×10^{-6} Torr, and the wall panels would be at a temperature of 80 K.

Typically hemispherical-angular and angular-hemispherical reflectance data are obtained from integrating sphere and hemiellipsoidal reflectometer measurements. These data frequently are used to determine radiative properties of participating media. Crosbie[17] has shown for an isotropically scattering medium with refractive index of unity and for a nonreflecting substrate that the two reflectances are reciprocal. A second objective of this paper was to show a numerical verification of this reciprocity for a radiatively participating medium for which the substrate has a nonzero reflectance and the medium refractive index is greater than unity.

Received Nov. 4, 1983; revision received March 16, 1984.

*Associate Professor, Department of Mechanical Engineering.
†Dean, School of Engineering, and Professor of Mechanical Engineering.

Statement of Problem

The geometry and coordinate system are shown in Fig. 1. Collimated radiant intensity I_0 is taken to be incident upon a two-layered medium consisting of a radiatively participating layer, the deposit, and an opaque substrate. The coating is considered to have smooth boundary interfaces. The top interface is considered to allow reflection and refraction governed by Snell's law and Fresnel's equations. The substrate is considered to be specular and reflect radiation according to Fresnel's equations. In Fig. 1, regions 1, 2, and 3 represent vacuum, deposit, and substrate, respectively. The interface reflectances ρ_{12} and ρ_{21} are not equal for equal incidence angles and must be considered separately. The substrate reflectance is designated as ρ_{23}. The deposit is taken to be absorbing and isotropically scattering with negligible emission.

The presence of the monodirectional incident flux requires the collimated intensity transmitted through the top interface to be handled as a source term within the radiative transport equation vs the boundary conditions. The collimated flux representation proposed by Kourganoff[18] was to define the incident intensity I_0 corresponding to the monodirectional flux such that its integrated value gives the correct incident flux. Such an expression is

$$I_0 = F_0\delta(\mu_1-\mu_1^*)\delta(\phi-\phi^*) \tag{1}$$

where $\delta(\mu_1-\mu_1^*)$ is the Dirac "selecting" function, μ_1^* is the cosine of the incidence angle of the monodirectional flux, μ_1 corresponds to the cosine of any angle of incidence, ϕ is the azimuthal angle, ϕ^* the azimuthal angle corresponding to the incident collimated flux, and F_0 the incident monodirectional flux normal to the projected area of the irradiated surface.

Kourganoff[18] proposed this representation because, from the properties of $\delta(\mu_1-\mu_1^*)$ and $\delta(\phi-\phi^*)$, it is easy to verify that Eq. (1) yields the correct description of the two main physical features of the incident radiation, that of being zero intensity for all directions μ and ϕ other than that of μ_1^* and ϕ^* and that of giving a flux $F_0\mu_1^*$ per unit of the radiated surface. The transport equation can be written for isotropic scattering as[11]:

$$\frac{dI}{d\tau} = -\frac{I}{\mu}+\frac{W}{4\pi\mu}\int_0^{2\pi}\int_{-1}^{1} I(\tau,\mu')\,d\mu'\,d\phi$$

$$+\frac{W}{4\pi\mu}\int_0^{2\pi}\int_0^{1} I^*(\tau,\mu^*)\,d\mu'\,d\phi \tag{2}$$

where W is the albedo, τ the optical thickness, $\mu=\cos\theta$, and θ the angle formed by the upward normal direction and the ray of radiative intensity, $I(\tau,\mu)$. In Eq. (2) the last term on the

right-hand side corresponds to the transmitted incident collimated radiation. This term represents the scatter into the reference beam, $I(\tau,\mu)$, out of the partially attenuated incident beam. Note that $I^*(\tau,\mu^*)$ represents the intensity of the incident radiation at any point τ within the deposit. Due to scattering and absorption the incident radiation is attenuated as it traverses through the deposit and no longer has the value I_0.

The expressions for the value of the attenuated intensity of the incident collimated radiation due to both absorption and scattering can be written as:

$$I^*(\tau,\mu^*)=\frac{\rho_{23}(\mu^*)[1-\rho_{12}(\mu_1^*)]n^2e^{-(\tau_0+\tau)/\mu^*}I_0}{[1-\rho_{21}(\mu^*)\rho_{23}(\mu^*)e^{-2\tau_0/\mu^*}]} \tag{3}$$

and

$$I^*(\tau,-\mu^*)=\frac{[1-\rho_{12}(\mu^*)]n^2e^{-(\tau_0-\tau)/\mu^*}I_0}{[1-\rho_{21}(\mu^*)\rho_{23}(\mu^*)e^{-2\tau_0/\mu^*}]} \tag{4}$$

Equation (2) can now be written in the form

$$\frac{dI}{d\tau}=\frac{-I}{\mu}+\frac{W}{2\mu}\int_{-1}^{1}I(\tau,\mu')d\mu'+\frac{W}{4\pi\mu}\int_0^{2\pi}\int_0^1 I^*(\tau,\mu^*)d\mu'd\phi$$
$$+\frac{W}{4\pi\mu}\int_0^{2\pi}\int_0^1 I^*(\tau,-\mu^*)d\mu'd\phi \tag{5}$$

where $I^*(\tau,\mu^*)$ and $I^*(\tau,-\mu^*)$ are given by Eqs. (3) and (4), respectively. The expression I_0 in Eqs. (3) and (4) is given by Eq. (1). Substitution of Eq. (1) into Eqs. (3) and (4), and then combining these with Eq. (5) yields

$$\frac{dI}{d\tau}=\frac{-I}{\mu}+\frac{W}{2\mu}\int_{-1}^{1}I(\tau,\mu')d\mu'+[I^*(\tau,\mu^*)+I^*(\tau,-\mu^*)]$$
$$\times\frac{W}{4\pi\mu}\int_0^{2\pi}\int_0^1 I_0d\mu'd\phi \tag{6}$$

In order to simplify Eq. (6), let the integral in the last term be evaluated. Therefore,

$$\int_0^{2\pi}\int_0^1 I_0d\mu d\phi=\int_0^{2\pi}\int_0^1 F_0\delta(\mu_1-\mu_1^*)\delta(\phi-\phi^*)d\mu d\phi \tag{7}$$

and recalling Shell's law,

$$\mu_1=[1-n^2(1-\mu^2)]^{1/2} \tag{8}$$

the differential $d\mu$ becomes

$$d\mu=\left(\frac{\mu_1}{\mu}\right)\frac{d\mu_1}{n^2} \tag{9}$$

Substitution of Eq. (9) into Eq. (7) gives

$$\int_0^{2\pi}\int_0^1 I_0d\mu d\phi=\frac{F_0}{n^2}\left(\frac{\mu_1^*}{\mu^*}\right) \tag{10}$$

Incorporating Eq. (10) into the transport equation, Eq. (6), yields the result

$$\mu\frac{dI}{d\tau}=-I+\frac{W}{2}\int_{-1}^{1}I(\tau,\mu')d\mu'+\{I^*(\tau,\mu^*)$$
$$+I^*(\tau,-\mu^*)\}\frac{WF_0}{n^24\pi}\left(\frac{\mu_1^*}{\mu^*}\right) \tag{11}$$

The next step is to multiply both sides of Eq. (11) by π/F_{in} and define

$$i(\tau,\mu)=\frac{\pi I(\tau,\mu)}{F_{in}};\quad F_{in}=F_0\mu_1^* \tag{12}$$

which yields

$$\frac{di}{d\tau}=\frac{-i}{\mu}+\frac{W}{2\mu}\int_{-1}^{1}i(\tau,\mu')d\mu'+\frac{W}{4\mu n^2}$$
$$\times\{I^*(\tau,\mu^*)+I^*(\tau,-\mu^*)\}\left(\frac{1}{\mu^*}\right) \tag{13}$$

Since simplification of the source term has been accomplished, Eq. (13) can be transformed into a system of differential equations by replacing the integral terms in Eq. (13) by a Gaussian quadrature[19] of the form

$$\int_{-1}^{1}f(\mu)d\mu\simeq\sum_{j=1}^{p}a_jf(\mu_j) \tag{14}$$

where μ_j are the ordinates, a_j the weighting factors, and p (an even integer) the order of the quadrature. Replacing the integral term in Eq. (13) by Eq. (14) yields a system of p simultaneous differential equations:

$$\frac{di}{d\tau}(\tau,\mu_\ell)=\frac{-i(\tau,\mu_\ell)}{\mu_\ell}+\frac{W}{2\mu_\ell}\sum_{j=1}^{p}i(\tau,\mu_j)a_j+\frac{W}{2\mu_\ell n^2}$$
$$\times\{I^*(\tau,\mu^*)+I^*(\tau,-\mu^*)\}\left(\frac{1}{\mu^*}\right)\quad \ell=1,\ldots,p \tag{15}$$

The value[19] of p used for these calculations was $p=40$; this corresponds to 20 positive and 20 negative μ directions.

Since the incident collimated flux has been used as a source term in the transport equation the boundary conditions do not involve the collimated radiation transmission through the top surface. Therefore, the normalized boundary conditions become

$$i(\tau_0,-\mu_\ell)=\rho_{21}(\mu_\ell)i(\tau_0,\mu_\ell)\quad \ell=1,\ldots,p/2 \tag{16}$$

and

$$i(0,\mu_\ell)=\rho_{23}(\mu_\ell)i(0,-\mu_\ell)\quad \ell=1,\ldots,p/2 \tag{17}$$

The solution of Eqs. (15-17) was accomplished numerically by the Milne predictor-corrector method.[20,21] Convergence was typically achieved within 3-5 iterations.

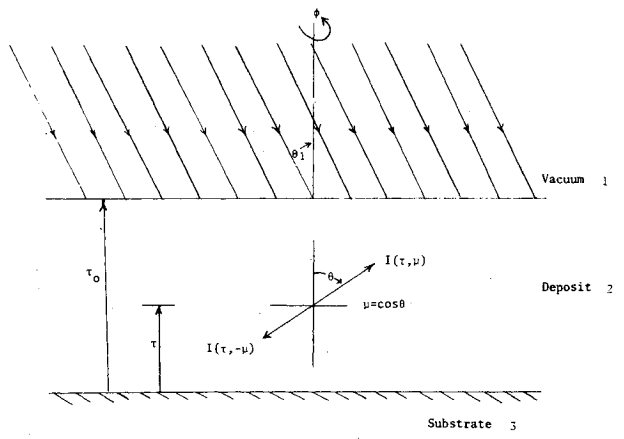

Fig. 1 Geometry and coordinate system.

The mathematical definition of biangular reflectance for this problem becomes

$$\rho_{ba}(\mu_1,\phi^*)=\pi I_r/F_{\text{in}} \tag{18}$$

where I_r is the reflected intensity, i.e.,

$$I_r=\rho_{12}(\mu_1^*)I_0+[1-\rho_{21}(\mu^*)]I^*(\tau_0,\mu^*)$$
$$+\{[1-\rho_{21}(\mu)]/n^2\}I(\tau_0,\mu) \tag{19}$$

Substituion of Eq. (19) into Eq. (18) along with the expression for I_0 and $I(\tau_0,\mu^*)$ yields

$$\rho_{ba}(\mu_1,\phi^*)=\pi\delta(\mu_1-\mu_1^*)\delta(\phi-\phi^*)\left\{\rho_{12}(\mu_1^*)\right.$$
$$\left.+\frac{[1-\rho_{21}(\mu^*)][1-\rho_{12}(\mu_1^*)]\rho_{23}(\mu^*)n^2e^{-2\tau_0/\mu^*}}{[1-\rho_{21}(\mu^*)\rho_{23}(\mu^*)e^{-2\tau_0/\mu^*}]}\right\}$$
$$+\frac{[1-\rho_{21}(\mu)]i(\tau_0,\mu)}{n^2} \tag{20}$$

The first term appears only when the specular angle is viewed. The last term is the diffuse term and has a contribution in all directions μ_1, where μ and μ_1 are related by Snell's law, Eq. (8). Now, by definition, let

$$\rho_{ba}^d(\mu_1)=\{[1-\rho_{21}(\mu)]/n^2\}i(\tau_0,\mu) \tag{21}$$

be the diffuse component of the biangular reflectance. It can be shown[13] that, for a bare substrate (no participating medium), the hemispherical-angular and angular-hemispherical reflectances are equal (reciprocal). Now the validity of this reciprocal correspondence will be demonstrated for the case of the substrate covered by an absorbing, scattering film. No conclusive proof is given since the results are in the form of numerical values, not closed-form functions. Reciprocity will be based upon comparison of numerical calculations of $\rho_{ha}(\mu_1)$ and $\rho_{ah}(\mu_1)$. From the expressions already presented, it easily can be shown in closed form that reciprocity is valid for $W=0$.

The expression for $\rho_{ah}(\mu_1^*)$ will now be developed in terms of the biangular reflection. The angular-hemispherical reflectance is defined by Hottel and Sarofim[22] as

$$\rho_{ah}(\mu_1^*)=\frac{1}{F_{\text{in}}}\int_0^{2\pi}\int_0^1 I_r\mu_1\,d\mu_1\,d\phi \tag{22}$$

Substitution of Eq. (19) into Eq. (22) yields

$$\rho_{ah}(\mu_1^*)=\rho_{12}(\mu_1^*)+\int_0^1\rho_{ba}^d(\bar{\mu}_1)d\bar{\mu}_1$$
$$+\frac{\rho_{23}(\mu_1^*)[1-\rho_{21}(\mu_1^*)][1-\rho_{21}(\mu^*)]e^{-2\tau_0/\mu^*}}{[1-\rho_{21}(\mu^*)\rho_{23}(\mu^*)e^{-2\tau_0/\mu^*}]} \tag{23}$$

where $\bar{\mu}_1=\sin^2\theta_1$. The integral term in Eq. (23) comes directly from Eq. (21) and the integration was performed numerically.

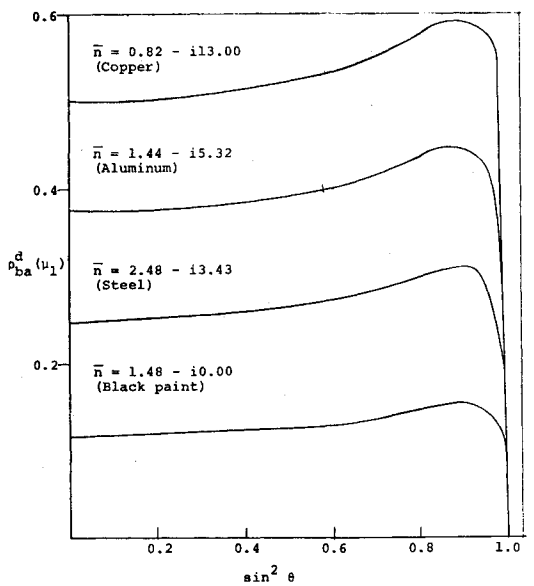

Fig. 2 Theoretical biangular reflectance distribution for a H_2O deposit; $W=1.0$, $\mu_1^*=1.0$, $n=1.2$.

Biangular Results

A plot of the diffuse component of the biangular reflectance vs $\sin^2\theta_1$ is illustrated in Fig. 2. The area under the curve represents the integral term in Eq. (23). This diffuse component is due to the internal scattering within the deposit. The incident flux was chosen as normally incident because axial symmetry has been assumed within the deposit. For a diffusely irradiated surface the assumption of axial symmetry is valid. However, for a monodirectional incident flux axial symmetry is probably not physically realistic except for small angles of incidence ($\mu_1^*\simeq 1$). Table 1 indicates a comparison of the calculated hemispherical-angular and angular-hemispherical reflectances for various substrates. The numerical agreement indicates that reciprocity appears to be reasonable.

Experimental biangular data have been presented in Ref. 14. The biangular measurements were within ±0.5% on two successive measurements for any zenith reflection angle; all details regarding angle measurement, deposition rate, etc., are documented in Ref. 14. It was attempted to achieve a cor-

Table 1 Comparison of hemispherical-angular and angular-hemispherical reflectance for various orders of quadrature at $n=1.2$, $W=1.0$, and $\mu_1^*=0.999$

Substrate	τ_0	50 steps, 10 point quadrature[a]	50 steps, 40 point quadrature[b]	100 steps, 40 point quadrature[b]	200 steps, 40 point quadrature[b]
Black paint $n=1.48-i0.00$	0.5	0.1563	0.1563	0.1496	0.1547
Steel $n=2.58-i3.43$	0.5	0.5005	0.4906	0.4902	0.5023
Aluminum $n=1.44-i5.32$	0.5	0.7438	0.7357	0.7220	0.7360
Copper $n=0.82-i13.00$	0.5	0.9610	0.9507	0.9412	0.9598

[a]Hemispherical-angular reflectance. [b]Angular-hemispherical reflectance.

respondence between the data and theory by using the radiative properties determined in Ref. 16. The data[14] are not a direct measure of the absolute value of biangular reflectance but rather only indicate the angular dependence of the biangular reflectance. The data[14] are given as the ratio of the detector output at any viewing angle with a deposit present to the detector output of the bare substrate in the specular direction. The detector output is proportional to the power incident on the detector. It is necessary to have expressions that correspond to the detector outputs with and without the deposits. It can be shown[14,23] that the ratio of detector outputs is given by

$$P_{D2}/P_{D1} \propto \rho^{d}_{ba}(\mu_1)\mu_1 \tag{24}$$

The proportionality constant could not be computed accurately, therefore, it was decided to investigate the general trend of the reflectance data with respect to viewing angle. Since the incidence angle is required to be small, as indicated earlier, the data at an angle of incidence of 0 deg, $\lambda = 0.9$ μm (wavelengh of radiation) and $d = 300$ μm (deposit thickness) were used. The radiative properties for the CO_2 deposit at $\lambda = 0.9$ μm are given in Ref. 16 as $n = 1.4$, $\sigma = 15$/cm, and $k \to 0$ or $\tau_0 = 0.45$. The magnitude in the normal direction was adjusted such that Eq. (24) and the data were identical at this point. This is equivalent to picking the proportionality constant in Eq. (24) to give the correct detector output ratio in the normal direction. The angular dependence of the data and theory are indicated in Fig. 3. The distributions of both the data and theory for the near normal incident flux correspond closely to a cosine profile which implies that although the substrate is specular and the interfaces reflect and transmit specularly, the internal scattering causes an essentially diffuse biangular reflection. The comparison of theory and data for the larger incidence angles (33, 55, and 66 deg) of the collimated incident flux shows that the assumption of axially symmetric radiative transport is not appropriate. The data at the large incidence angles are seen to deviate substantially from the theoretical profiles. It is believed that the assumption of axial symmetry is the primary cause for this disagreement between theory and data. Although some degree of anisotropic scattering exists, it is not believed that anisotropic scattering is the primary reason for the disagreement between the theory and data. Usually anisotropic scattering in a multiple-scattering medium is dominant only for the optically thin case ($\tau_0 < 0.1$); here the optical thickness $\tau_0 = 0.45$. For this optical thickness the effects of multiple scattering will lessen the importance of a nonisotropic phase function. Also as the incidence angle increases to larger angles the effective optical path increases significantly above $\tau_0 = 0.45$. Finally, the structure of the deposit is amorphous. Thus, the voids in the deposit, which cause the scattering, are a random collection of various sizes of irregular shapes. The net effect of these irregular sizes and shapes is to yield an effective phase function which approaches being isotropic. Thus, one should be careful in assuming axial symmetry for a collimated flux incident at angles that are not near zero. It is planned to model the case of nonaxial symmetry to determine if the agreement with data is improved. It is believed that it is the axial-symmetry assumption and not the isotropic phase function assumption which primarily caused the disagreement in Fig. 3 at high incidence angles.

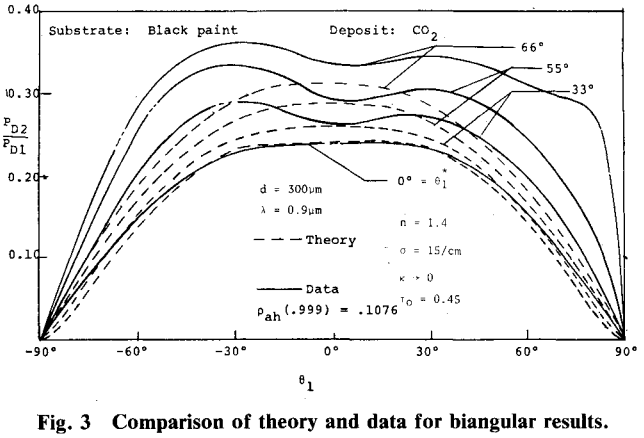

Fig. 3 Comparison of theory and data for biangular results.

Summary and Conclusions

An analytical formulation of the biangular reflectance of an absorbing and scattering coating was presented and results were compared with experimental data. The agreement between theory and data was shown to be very good for near normal angles of incidence. However for non-near normal incidence angles the general trends of the theory and data did not agree. Also it was shown that the reciprocity between the hemispherical-angular and angular-hemispherical reflectance appears to be valid for an absorbing and scattering medium for near-normal incidence angles. It is recommended that the assumption of axial symmetry be eliminated and then to determine if the analytical model and data show better agreement for high incidence angles.

References

[1]Hsia, H. M. and Love, T. J., "Radiant Heat Transfer Between Parallel Plates Separated by a Nonisothermal Medium with Anisotropic Scattering," *Journal of Heat Transfer*, Vol. 89, Sec. C, Aug. 1967, pp. 197-203.

[2]Chandrasekhar, S., *Radiative Transfer*, Dover Publications, New York, 1960.

[3]Hottel, H. C., Sarofim, A. F., Evans, L. B., and Vasalos, I. A., "Radiative Transfer in Anisotropically Scattering Media: Allowance for Fresnel Reflection at the Boundaries," *Journal of Heat Transfer*, Vol. 90, Sec. C, Feb. 1968, pp. 56-62.

[4]Callis, L. B., "The Radiative Transfer Equation and Environmental Effects in the Upper Atmosphere," AIAA Paper 72-663, June 1972.

[5]Wolf, P., "An Analytical and Experimental Study of the Radiant Heat Transfer in Scattering, Absorbing, and Emitting Media," Ph.D. Dissertation, University of Tennessee, 1968.

[6]Merriam, R. L., "A Study of Radiative Characteristics of Condensed Gas Deposits on Cold Surfaces," Ph.D. Dissertation, Dept. of Mechanical Engineering, Purdue University, W. Lafayette, In., 1968.

[7]Roux, J. A., Todd, D. C., and Smith, A. M., "Eigenvalues and Eigenvectors for Solutions to the Radiative Transport Equation," *AIAA Journal*, Vol. 10, July 1972, pp. 973-976.

[8]Roux, J. A. and Smith, A. M., "Comparison of Three Solution Techniques for Solving the Radiative Transport Equation," *Progress in Astronautics and Aeronautics: Thermophysics and Spacecraft Control*, Vol. 35, edited by R. G. Hering, AIAA, New York, 1974, pp. 3-22.

[9]Sparrow, E. M., and Cess, R. D., *Radiation Heat Transfer*, Brooks/Cole Publishing Company, Belmont, Calif., 1966.

[10]Love, T. J., *Radiative Heat Transfer*, Charles E. Merrill Publishing Company, Columbus, Ohio, 1968.

[11]Ozisik, M. N., *Radiative Transfer*, John Wiley & Sons, New York, 1973.

[12]Edwards, D. K., *Radiation Heat Transfer Notes*, Hemisphere Publishing Corp., New York, 1981.

[13]Siegel, R. and Howell, J. R., *Thermal Radiation Heat Transfer*, 2nd Ed., Hemisphere Publishing Corp., New York, 1981.

[14]Smith, A. M. and Wood, B. E., "Bidirectional Reflectance of Specular and Diffusing Surfaces Contaminated with CO_2 Cryofilms," *Thermophysics of Spacecraft and Outer Planet Entry Probes, Progress in Astronautics and Aeronautics*, Vol. 56, edited by A. M. Smith, AIAA, New York, 1977, pp. 157-173.

[15]Mills, D. W. and Smith, A. M., "Effects of Reflections from CO_2 Cryopanel Deposits on the Thermal Balance of a Test Model in a Space Simulation Chamber," *Journal of Spacecraft and Rockets*, Vol. 7, March 1970, pp. 374-376.

[16]Roux, J. A. and Smith, A. M., "Determination of Radiative Properties from Transport Theory and Experimental Data," *Spacecraft Radiative Transfer and Temperature Control, Progress in Astronautics and Aeronautics*, Vol. 83, edited by T. E. Horton, AIAA, New York, 1982, pp. 22-37.

[17]Crosbie, A. L., "Reflection Function of an Isotropically Scattering Medium," *AIAA Journal*, Vol. 11, Oct. 1973, pp. 1448-1449.

[18]Kourganoff, J., *Basic Methods in Heat Transfer Problems*, Dover Publications, New York, 1964.

[19]Abramowitz, M. and Stegum, I. A., *Handbook of Mathematical Functions*, Government Printing Office, Washington, 1967.

[20]Tenenbaum, M. and Pollard, H., *Ordinary Differential Equations*, Harper and Row, New York, 1963.

[21]Scarborough, J. B., Numerical Mathematical Analysis, 5th Ed., The John Hopkins Press, Baltimore, Md., 1962.

[22]Hottel, H. C. and Sarofim, A. F., *Radiative Transfer*, McGraw-Hill Book Co., New York, 1967.

[23]Roux, J. A., "Radiation Heat Transfer of Coatings on a Cryogenic Surface," AEDC-TR-71-90, April 1971.